Lattice Thermal Conductivity of Germanium-Silicon Alloy Single Crystals at Low Temperatures*

ARNOLD M. TOXEN
International Business Machines Research Center, Yorktown, New York and Cornell University, Ithaca, New York

(Received December 9, 1960)

Thermal conductivity measurements are reported for five single-crystal Ge-Si specimens containing 0–7.56 at. % Si. The measurements were made under steady-state conditions and cover the temperature range 2–50°K. The experimental results are compared to three theoretical models, those of Berman *et al.*, Callaway, and Klemens; it is found that the data are best fit by Callaway's model. Good agreement between experimental results and theoretical models is obtained by postulating only three sources of phonon scattering in the specimens: three-phonon processes, isotopic point-defect scattering by the germanium and silicon atoms, and boundary scattering. However, evidence is presented that boundary scattering occurs not only at the external surfaces of the specimens, but also at internal surfaces associated with microscale fluctuations of composition of the type reported by Goss, Benson, and Pfann.

I. INTRODUCTION

THE purpose of this experiment was the study of the effect upon lattice thermal conductivity of the scattering of phonons by point defects. These are defects whose linear dimensions are much less than the wavelengths of the important phonons, i.e., $L \ll (\theta/T)a$, where L is any dimension of the defect, θ is the Debye temperature, T is the absolute temperature, and a is the lattice parameter. At 20°K, θ/T is approximately 20 in germanium. One way to study the point-defect scattering is to modify the defect concentration in a known way and measure the resultant change in thermal conductivity. In this experiment, the materials studied were single crystals of germanium-silicon alloys, which contained 0 to 7.56 at. % Si. In this alloy system, the silicon atoms, which differ from the germanium atoms in mass, size, and chemical bonding, constitute point defects in the host germanium lattice. Klemens[1] has discussed the phonon scattering cross section of point defects; on the basis of Klemens' formulas, the author has estimated that the mass difference between silicon and germanium accounts for about 99% of the scattering cross section for a silicon atom in the germanium lattice. Hence in alloys of germanium with silicon, the silicon atoms may be considered, to a first approximation, as isotopes of germanium. Naturally occurring germanium itself consists of five isotopes. Therefore, the germanium atoms differ in mass from each other. Because any departure from perfect periodicity in the lattice causes phonon scattering, the germanium atoms scatter phonons—they are isotopic point defects. The germanium-silicon alloy system was chosen for this study for the following reasons: First, the materials are simple insulators at low temperatures, having no electronic contribution to the thermal conductivity; hence the conduction of heat is entirely by lattice vibrations, i.e., phonons. Secondly, crystals which contain relatively few dislocations and chemical impurities can be grown. And thirdly, the silicon atoms are a particularly simple type of point defect, primarily differing from the germanium atoms in mass. Three theoretical models are considered—those of Klemens,[1,2] Berman *et al.*,[3] and Callaway.[4] All of these models relate the thermal conductivity to the scattering of phonons by various mechanisms.

In Sec. II of this paper the experimental details are briefly described. Section III contains descriptions of the three theoretical models considered in this paper. In Sec. IV is contained the discussion of the theoretical models and their comparison to the experimental results. Section V contains a summary of the conclusions. Finally, in the Appendix is a description and discussion of the microstructure found in the alloy specimens.

II. EXPERIMENTAL DETAILS

The alloy crystals, which were very kindly supplied by S. M. Christian of the RCA Research Laboratories, were $\frac{1}{8}$ in.$\times\frac{1}{8}$ in.$\times\frac{5}{8}$ in. in size. The compositions are tabulated in Table I and were determined by the author from density and x-ray lattice parameter measurements. The uncertainties stated are those estimated from the

TABLE I. Specimen characteristics.

Specimen	Composition	$10^4\Gamma$	$10^{44}A$ (sec^3)
1	Ge	5.72	2.40
2	Ge+0.77 at. % Si	34.6	12.9
3	Ge+4.23 at. % Si	166.	65.1
4	Ge+7.25 at. % Si	282.	108.
5	Ge+7.56 at. % Si	294.	116.

* The experimental work reported in this paper is part of a thesis submitted in partial fulfillment of the requirements of the degree of Doctor of Philosophy at Cornell University and was supported in part by a grant from the National Science Foundation.

[1] P. G. Klemens, Proc. Phys. Soc. (London) **A68**, 1113 (1955).

[2] P. G. Klemens, Proc. Roy. Soc. (London) **A208**, 108 (1951).

[3] R. Berman, P. T. Nettley, F. W. Sheard, A. N. Spencer, R. W. H. Stevenson, and J. M. Ziman, Proc. Roy. Soc. (London) A253, 403 (1959).

[4] Joseph Callaway, Phys. Rev. **113**, 1046 (1959).

precision of the two measurements. The manner in which the specimens were mounted is as follows. One end of the specimen is soldered with indium to an electrical heater, the other end to a heat sink whose temperature can be varied. A one-dimensional steady heat flow is set up along the specimen by means of the heater, and two carbon resistance thermometers mounted on the central region of the crystal measure the temperature gradient. The entire assembly is then mounted in a vacuum chamber. The thermal conductivity K can then be calculated from the power, Q, carried by the specimen; the temperature difference, ΔT, of the thermometers; the separation of the thermometers, Δl; and the cross sectional area of the specimen, S. The relationship is simply $K=Q\Delta l/S\Delta T$. The thermal conductivity measurements were carried out over the temperature range 2–50°K. The uncertainty in the temperature measurements is approximately 1% for temperatures below 30°K and 1–2% for temperatures above 30°K. The uncertainty in the measured values of thermal conductivity is estimated to be less than or equal to the following values: ±5% in the temperature range 4–30°K; ±5 to 10% in the temperature range below 4°K, the error increasing with decreasing temperature; and ±5 to 10% in the temperature range 30–50°K, the error increasing with increasing temperature.

III. THEORETICAL MODELS

First consider the results of Klemens,[1] who found the scattering time τ_I, due to isotopic point defects to be given by

$$\frac{1}{\tau_I}=\left[\frac{V_0}{4\pi c^3}\sum_i f_i(1-m_i/\bar{m})^2\right]\omega^4=A\omega^4. \tag{1}$$

In Eq. (1), c is the sound velocity; V_0, the atomic volume; m_i, the mass of the ith species of atom; f_i, the atomic fraction of the ith species of atom; $\bar{m}$ is the average atomic mass which is equal to $\sum_i f_i m_i$; and ω is the phonon frequency. A similar expression was suggested somewhat earlier by Pomeranchuk.[5] The frequency dependence is, of course, the same as that obtained in the classical Rayleigh treatment. If the scattering time defined by Eq. (1) is inserted into the expression for the thermal conductivity,[2,4]

$$K=\frac{k}{2\pi^2 c}\int_0^{k\theta/\hbar}\tau\frac{\hbar^2\omega^2}{k^2T^2}\frac{e^{\hbar\omega/kT}}{(e^{\hbar\omega/kT}-1)^2}\omega^2 d\omega, \tag{2}$$

where k is Boltzman's constant, and $\hbar$ is Planck's constant divided by 2π, then the resulting integral diverges at the lower limit. Physically, this occurs because the relaxation times for the low-frequency phonons become very large, giving rise to a very large conductivity. Klemens[2] presents arguments to show that, because of the influence of the nonresistive 3-phonon processes (the momentum-conserving N processes), the impurity scattering time τ_I should be modified at low frequencies in the following way:

$$\begin{aligned} 1/\tau_I&=A\omega^4, && \omega>kT/\hbar;\\ 1/\tau_I&=A(kT/\hbar)^4, && \omega<kT/\hbar. \end{aligned} \tag{3}$$

If this modified expression for τ_I is inserted into Eq. (2), the resulting thermal conductivity is given by

$$K_I=\frac{k}{2\pi^2 c}\frac{1}{A(kT/\hbar)}\left[\int_0^1\frac{x^4e^x dx}{(e^x-1)^2}+\int_1^{\theta/T}\frac{e^x dx}{(e^x-1)^2}\right]. \tag{4}$$

For $\theta/T\gg 1$, the second integral is a constant and K_I is inversely proportional to T. In any real crystal with finite boundaries, phonons are scattered at the boundaries, giving an upper limit to the total relaxation time. Hence the conductivity must always be finite. This problem was first treated by Casimir,[6] who obtained a relaxation time for boundary scattering of the form $1/\tau_B=c/L$ where L is a length characteristic of the size of the specimen and c is the velocity of sound. Combining the boundary scattering with Klemens' relation for point-defect scattering, the resultant scattering time is

$$\begin{aligned} 1/\tau&=c/L+A\omega^4, && \omega>kT/\hbar;\\ 1/\tau&=c/L+A(kT/\hbar)^4, && \omega<kT/\hbar. \end{aligned} \tag{5}$$

Substituting Eq. (5) into Eq. (2) gives for the thermal conductivity,

$$K=\frac{k}{2\pi^2 c}\frac{1}{A(kT/\hbar)}\left[\frac{1}{1+(c/LA)(\hbar/kT)^4}\int_0^1\frac{x^4e^x dx}{(e^x-1)^2}+\int_1^\infty\frac{1}{1+(c/LA)(\hbar/kT)^4x^{-4}}\frac{e^x dx}{(e^x-1)^2}\right]. \tag{6}$$

The model by Berman *et al.* differs from the other two under consideration in that it is based on a variational calculation of the phonon mean free path. This calculation includes the effects of three-phonon processes and isotopic point defects, but does not include the effects of boundary scattering. Hence the model is not applicable at temperatures below that of the thermal conductivity maximum and at all temperatures represents an upper bound to the thermal conductivity. By substituting the expression derived by Berman *et al.* for the average phonon mean free path into the kinetic formula, $K=C_v cl/3$, which relates the thermal conductivity K to the lattice specific heat C_v, the phonon velocity c, and the average mean free path l, one obtains the following expression for the thermal conductivity:

$$K=\frac{0.042c^2C_v}{6\pi\gamma}\left(\frac{\theta}{T}\right)^3\left(\frac{\hbar c}{kT}\right)\left(\frac{M}{\pi\Gamma kT}\right)^{\frac{1}{2}}. \tag{7}$$

[5] I. Pomeranchuk, J. Phys. U.S.S.R. **6**, 237 (1942).

[6] H. B. G. Casimir, Physica **5**, 495 (1938).

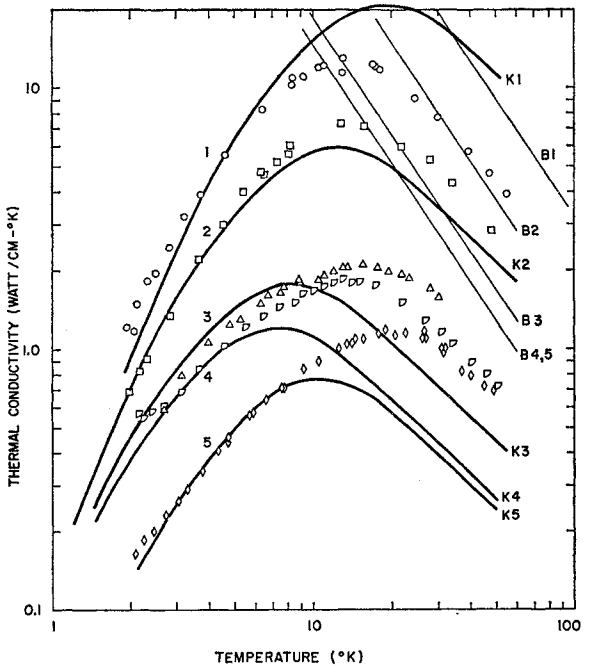

FIG. 1. Thermal conductivity: Data points 1, 2, 3, 4, 5 are measured for specimens 1 through 5 listed in Table I. Corresponding to these compositions are curves $K1$, $K2$, $K3$, $K4$, and $K5$ calculated from Klemens' model. Also corresponding to these compositions are curves $B1$, $B2$, $B3$, $B4$, $B5$ calculated from the model of Berman *et al.* with the Grüneisen constant assumed equal to 0.71. See Sec. IV of the text.

In this expression, M is the atomic mass; Γ is the quantity $\sum_i f_i(1-m_i/\bar{m})^2$ which has appeared in Eq. (1) and Table I, and γ is the Grüneisen constant. Equation (7) is further simplified if we substitute for C_v the low-temperature limit of the Debye specific heat expression, $C_v=1944(T/\theta)^3$ joules/mole-deg. This results in the following expression:

$$K=\frac{0.179\hbar c^3}{\gamma(kT)^{\frac{3}{2}}}\left(\frac{M}{\Gamma}\right)^{\frac{1}{2}}. \tag{8}$$

The third theoretical model used was that by Callaway,[4] in which point defects, boundary scattering, and 3-phonon processes are included. Callaway's expression for the thermal conductivity is

$$K=\frac{k}{2\pi^2 c}(I_1+\beta I_2)=K_1+K_2, \tag{9}$$

where

$$I_1=\int_0^{k\theta/\hbar}\tau_c\frac{\hbar^2\omega^2}{k^2T^2}\frac{e^{\hbar\omega/kT}}{(e^{\hbar\omega/kT}-1)^2}\omega^2 d\omega, \tag{10}$$

$$I_2=\int_0^{k\theta/\hbar}\tau_c/\tau_n\frac{\hbar^2\omega^2}{k^2T^2}\frac{e^{\hbar\omega/kT}}{(e^{\hbar\omega/kT}-1)^2}\omega^2 d\omega, \tag{11}$$

and

$$\beta=\int_0^{\theta/T}\frac{\tau_c}{\tau_n}\frac{x^4e^x dx}{(e^x-1)^2}\Big/\int_0^{\theta/T}\frac{1}{\tau_n}\left(1-\frac{\tau_c}{\tau_n}\right)\frac{x^4e^x dx}{(e^x-1)^2}. \tag{12}$$

In Eqs. (10), (11), and (12), τ_c is the combined relaxation time defined by

$$1/\tau_c=A\omega^4+B_1T^3\omega^2+B_2T^3\omega^2+c/L. \tag{13}$$

The quantity τ_n is the relaxation time for momentum-conserving 3-phonon processes (N processes) and is of the form

$$1/\tau_n=B_2T^3\omega^2, \tag{14}$$

where B_2 is a constant.

In the right-hand side of Eq. (13), we can identify the first term as the reciprocal scattering time due to point defects. The second term represents the reciprocal scattering time caused by Umklapp processes; the third term is due to N processes, and the last term results from boundary scattering.

IV. DISCUSSION OF THE THEORETICAL MODELS AND THEIR COMPARISON WITH THE EXPERIMENTAL RESULTS

The thermal conductivity data are shown in Figs. 1–4. In each figure, the data points reading from top to bottom are for specimens 1–5, respectively. For comparison, curves are shown which have been calculated from theoretical models by Klemens, Berman *et al.*, and Callaway. In Fig. 1 are shown the curves calculated from Klemens' model, denoted $K1$ through

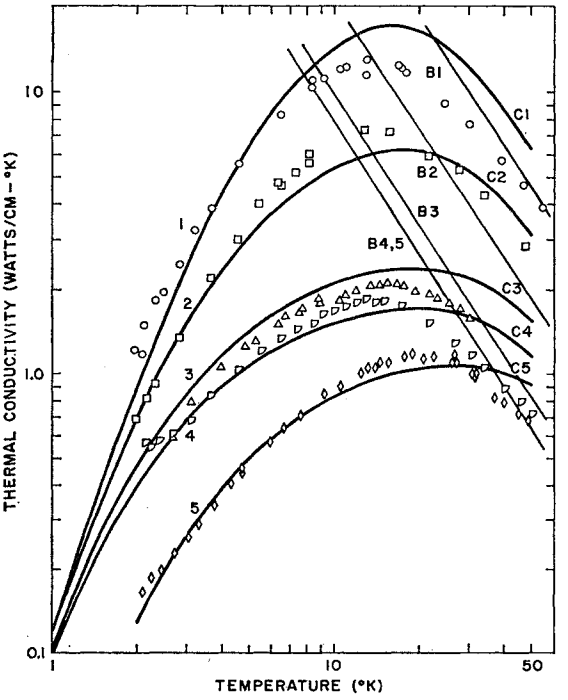

FIG. 2. Thermal conductivity: Data points 1, 2, 3, 4, 5 are defined as in Fig. 1. The calculated curves corresponding to these data points, $C1$–$C5$, respectively, were computed from Callaway's model with B_1+B_2 set equal to 2.77×10^{-23} sec/°K^3. Also corresponding to specimens 1 through 5 are curves $B1$, $B2$, $B3$, $B4$, $B5$ calculated from the model of Berman *et al.* with the Grüneisen constant set equal to 1.42.

$K5$ to correspond to the specimens. Shown in Figs. 1 and 2 are the curves calculated from the model of Berman *et al.*, designated $B1$ through $B5$ to correspond to the five samples. In Figs. 2, 3, and 4 are shown curves calculated from the model of Callaway and denoted $C1$ through $C5$ to correspond to samples 1 through 5, respectively.

Consider first the thermal conductivity curves which were calculated from Klemens' model. Equation (6) has been numerically integrated by Slack,[7] and it is his integrated results which were used to calculate curves $K1$ through $K5$. The calculations were made as follows: The value for c, the average phonon velocity, was taken to be 3.50×10^5 cm/sec.[8] The quantity A was calculated from Klemens' expression for the isotopic scattering time given in Eq. (1), using the measured silicon concentration, the measured atomic volume, and the known isotopic constitution of germanium and silicon. It was thus assumed that all the point-defect scattering of phonons by silicon and germanium atoms can be accounted for by the mass variation of the atoms. In addition it was assumed that the phonon velocity c varies inversely as the square root of the average atomic mass, $\bar{m}$. The values for A are given in Table I.

The quantity L was calculated from the specimen dimensions using the Casimir model,[6] i.e., $\pi(L/2)^2$ is

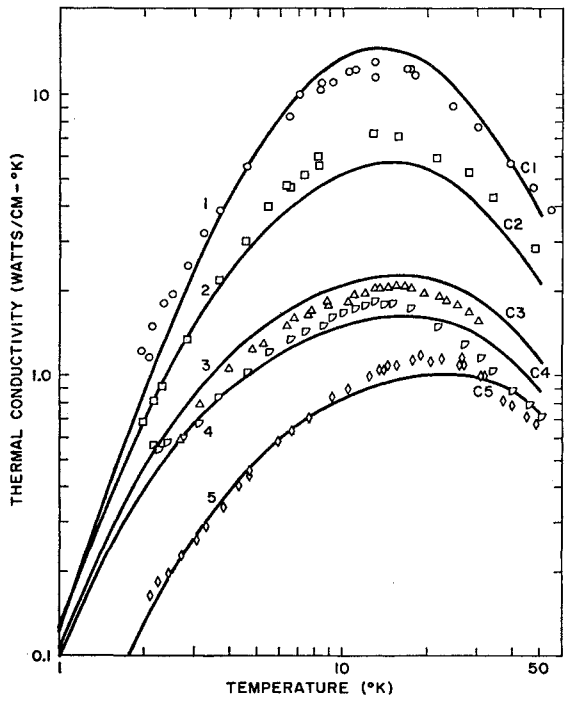

FIG. 3. Thermal conductivity: Data points 1, 2, 3, 4, 5 are defined as in Fig. 1. The calculated curves corresponding to these data points, $C1$–$C5$, respectively, were computed from Callaway's model with B_1+B_2 set equal to 5.54×10^{-23} sec/°K³. See text for details.

[7] G. A. Slack, Phys. Rev. **105**, 832 (1957).
[8] T. H. Geballe and G. W. Hull, Phys. Rev. **110**, 773 (1958).

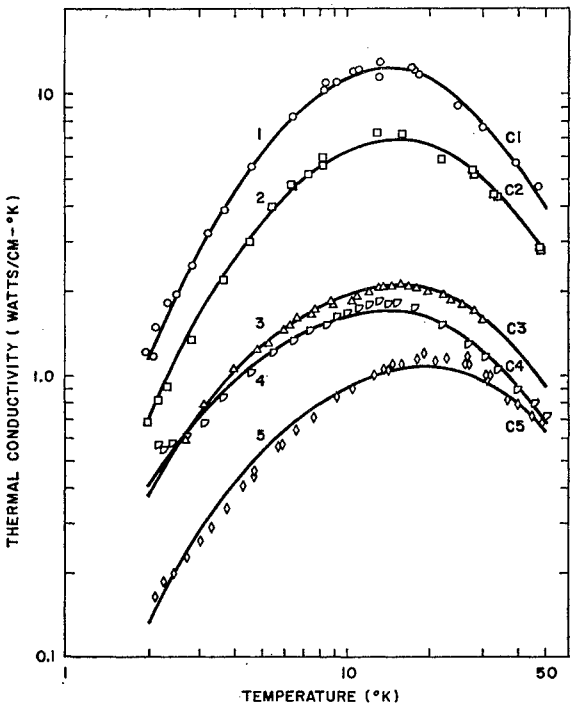

FIG. 4. Thermal conductivity: Data points 1, 2, 3, 4, 5 are defined as in Fig. 1. The curves are calculated from Callaway's model with the parameters given in Table II.

set equal to the cross-sectional area of the specimens. In this way, c/L was calculated to be 0.94×10^6 sec^{-1}. In the low-temperature region, $T<8$°K, the Klemens' model predicts quite well the magnitude and temperature dependence of the thermal conductivity data. Although $\tau_B=L/c$ had to be decreased by a factor of five from that value calculated from the specimen dimensions in order to fit the experimental data for specimen No. 5, this procedure seems quite warranted in view of the evidence for the existence in this specimen of internal boundaries associated with large microscale fluctuations in composition. This evidence is discussed in the Appendix. Because of the good fit between Klemens' model and the experimental data in this temperature region, it seems reasonable to conclude that the relevant assumptions made in deriving the model are applicable. Hence one may conclude that the Debye expression for the phonon specific heat is a good approximation, that the boundary scattering time, $\tau_B=L/c$, is substantially correct, and finally, that the silicon and germanium atoms scatter phonons as isotopic point defects, i.e., $1/\tau_I=A\omega^4$. These conclusions, however, are independent of the cutoff mechanism assumed by Klemens [see Eq. (3)], for in this temperature region one calculates the same results from Callaway's model (see Figs. 2, 3, and 4), or even from Klemens' expressions without the cutoff; if one substitutes $1/\tau=c/L+A\omega^4$ into Eq. (2), one gets the same values in the low-temperature region as with the relaxation time of

Eq. (3). In the high-temperature region, on the other hand, the Klemens model gives a poor fit to the data. The predicted conductivity for pure Ge at 30°K is too high by a factor of two. The predicted values of thermal conductivity for the alloy samples are too low. For example, the conductivities predicted for the 7% Si samples at 30°K are too low by a factor greater than two. One does not improve the fit by altering the value of τ_I from that given by Eq. (1). For if τ_I is increased to obtain agreement with the data in the range 30–50°K, the fit in the low-temperature region is worsened. If then τ_B is altered to restore the low-temperature fit, the fit in the region of the maximum is poor. Clearly, the use of the cutoff in the point-defect relaxation time does not seem to be the correct way to take account of three-phonon processes. When Callaway's model is discussed, it will be clear that there is a better way to handle three-phonon processes in this type of model.

Next, consider the calculations by Berman *et al.* Since these calculations do not include the effects of boundary scattering, they are not applicable at temperatures below that at which the conductivity maximum occurs. In Figs. 1, 2 are shown curves B_1 through B_5, corresponding to specimens one through five, which have been calculated from Eq. (8). To calculate K from Eq. (8), one must know γ. The Grüneisen theory of thermal expansion[9] gives

$$\gamma = (3\alpha V_m / C_p K_s), \tag{15}$$

where α is the linear coefficient of expansion, C_p is the specific heat at constant pressure, V_m is the molar volume, and K_s is the adiabatic compressibility. If one calculates γ from Eq. (15), one meets with difficulties for materials having the diamond lattice structure, e.g., Ge, Si, and InSb. For these materials, γ is not a constant but is a rapidly decreasing function of temperature for temperatures lower than about $\theta/3$; and for some of these materials even becomes negative.[10] For Ge, γ decreases rapidly below 120°K, but is approximately constant and equal to 0.71 for a wide temperature range above 200°K. This value was used to calculate K in Fig. 1 although its use is arbitrary. Had smaller values for γ been used, e.g., $\gamma=0.049$ at 40°K, the agreement of Eq. (8) with the data would have been far worse. In every case, the curves of Berman *et al.* give values for the thermal conductivity which are too high. At 40°K the conductivities calculated from Berman *et al.* differ from the experimental measurements by a factor which varies from 0.92 for specimen No. 2 to 2.2 for specimen No. 5. If, instead of calculating γ from thermal expansion data, one treated γ as a parameter to be determined from the thermal conductivity measurements, better agreement between the Berman *et al.* model and the experimental data can be obtained using γ equal to 1.42. Curves calculated in this manner are shown in Fig. 2.

In Figs. 2–4 are shown the curves calculated on the IBM 704 from the model of J. Callaway.[4] In this model, we have the constants c, c/L, and A which appear in the Klemens formula. In addition, however, we have the quantities B_1 and B_2 which are associated with three-phonon processes. As Callaway did, we assume B_1 and B_2 to be temperature independent. (Actually, if one allows B_1 to vary exponentially with temperature, as might be expected, no better agreement with the data is obtained.)

Callaway fitted Eq. (9) to the data of Geballe and Hull[7] for the thermal conductivity of ordinary germanium and isotopically enriched germanium. In this calculation, Callaway estimated that βI_2 was small compared to I_1 for the ordinary Ge and he neglected βI_2 in the calculation for the enriched Ge.

The quantity L, Callaway calculated from the low-temperature limit of the thermal conductivity of the enriched Ge specimen. For the sample 0.13 cm×0.157 cm in cross section, he obtained $L=0.180$ cm. Using this value for L, Callaway, by fitting Eq. (9) to the thermal conductivies of the two specimens, obtained his best fit for (B_1+B_2), assumed temperature independent, equal to 2.77×10^{-23} sec/°K^3 and a value of A of 2.57×10^{-44} sec^3 for the ordinary Ge. This value for A is in very good agreement with 2.40×10^{-44} sec^3 calculated from Klemens' formula, given by Eq. (1).

In Figs. 2 and 3, curves $C1$ through $C5$ have been calculated from Eq. (9) using the values for c/L and A previously used with Klemens' model. In Fig. 2 the value for B_1+B_2 was taken to be 2.77×10^{-23} sec/°K^3, the value selected by Callaway to fit the data of Geballe and Hull. In the low-temperature region, the curves are nearly identical to those calculated from Klemens' model and fit the data well. At high temperatures, the curves fit the experimental data much better than the corresponding Klemens curves, and predict the change in curve shape (broadening) as A is increased. The fit to the 0.77% Si sample is excellent. For the pure Ge sample, the Callaway calculation with B_1+B_2 equal to 2.77×10^{-23} sec/°K^3 gives too high a conductivity in the high-temperature region, the measured value being about 37% lower than the calculated value at 30°K. For the samples containing 7% Si, the experimental and calculated curves intersect, i.e., the theoretical temperature dependence is not quite correct in the temperature region 10–50°K. If one picks for B_1+B_2 a value larger than that selected by Callaway, the agreement between calculations and experimental data is improved. As can be seen in Fig. 3, (B_1+B_2) set equal to 5.54×10^{-23} sec/deg^3 gives a reasonably good fit to all of the experimental data.

It is possible to obtain agreement between the Callaway model and the experimental data better than that indicated in Fig. 3 by varying the quantities A, (B_1+B_2), and c/L. In Fig. 4 are shown theoretical

[9] See for example, J. C. Slater, *Introduction to Chemical Physics* (McGraw-Hill Book Company, Inc., New York, 1939).
[10] D. F. Gibbons, Phys. Rev. **112**, 136 (1958).

TABLE II. Parameters of Callaway model giving the best fit to the experimental data.

Sample	$10^{44}A_{exp}$ (sec^3)	$10^{23}(B_1+B_2)_{exp}$ (sec/°K^3)	$10^{-6}(c/L)$ exp (sec^{-1})	A_{exp}/A_{calc}
Ge	5.0	4.0	0.63	2.1
Ge+0.77 at. % Si	11.0	4.6	0.94	0.85
Ge+4.23 at. % Si	60.0	8.8	1.3	0.92
Ge+7.25 at. % Si	94.0	11.1	0.94	0.87
Ge+7.56 at. % Si	100.0	10.0	4.7	0.86

curves based upon Callaway's model which were fitted to the experimental data. The parameters chosen are shown in the second, third, and fourth columns of Table II. In the fifth column is shown the ratio of the value for A giving the best fit to the data to the value for A calculated from Eq. (1). From Table II, come the following observations:

(1) The values of A_{exp} obtained by curve fitting, are, with the exception of the Ge specimen, in excellent agreement with those calculated from Klemens' expression (see Table I). As the last column of Table II indicates, for the alloy specimens, A_{exp} is 8–15% smaller than A_{calc}. The fact that A_{exp} is smaller than A_{calc} is also consistent with the evidence presented in the Appendix to show that the silicon concentration is not uniform throughout the specimens. The fact that A_{exp}/A_{calc} is approximately equal to two for the Ge specimen is difficult to satisfactorily explain. Comparison of the thermal conductivity of the germanium specimen to other published results for high-purity germanium reveals the nature of the problem. For example, thermal conductivity data reported by Carruthers and others[11] are about 24% higher than those reported here for the temperature range 25–50°K. The results below 15°K are in good agreement, however. The discrepancy in the high-temperature region is higher than the estimated experimental error, implying either an unknown systematic error in the high-temperature data for that specimen or an unknown scattering mechanism present. Since spectroscopic analysis of the germanium specimen reveals 10 ppm of copper, 10 ppm of aluminum, and 5 ppm of magnesium, it is believed that the discrepancy is caused by some additional scattering mechanism associated with the electrically active impurities. It has been shown by various workers[11,12,13] that concentrations of one part per million of electrically active impurities have a significant effect on the low-temperature lattice thermal conductivity.

(2) The values obtained for B_1+B_2 increase with increasing silicon concentration. In Fig. 5 are plotted the experimental values of (B_1+B_2) as a function of silicon concentration. Although the scatter in the data is large, (B_1+B_2) seems to increase linearly with silicon concentration. Since 3-phonon processes, of which (B_1+B_2) is a measure, arise from contributions to the interatomic potential which are cubic in atomic displacements, one might conclude that the Ge–Si bond has a higher anharmonic content than does the Ge–Ge bond. On the other hand, the variation of B_1+B_2 with silicon concentration may be an indication that the model is not quite correct.

(3) With the exception of the 7.56 at. % Si specimen, all of the c/L values lie within about 30% of the value calculated from the Casimir model. It is quite likely that the large value of c/L obtained for the 7.56 at. % Si crystal can be attributed to the presence of large microscale fluctuations in silicon concentration. This point is discussed in some detail in the Appendix. It is also likely that the presence of these microscale fluctuations in the 4.23 at. % Si accounts for the 30% deviation of its c/L value from the results for 0.77 at. % Si and 7.25 at. % Si. The low value of c/L for the Ge specimen may be explained if one assumes that some fraction of the phonons incident upon the specimen's boundaries are specularly reflected. This effect has previously been reported in diamond[14] and sapphire.[15] On the basis of the model of Berman, Simon, and Ziman,[14] which corrects the Casimir model to include specular boundary scattering, 20% of the boundary

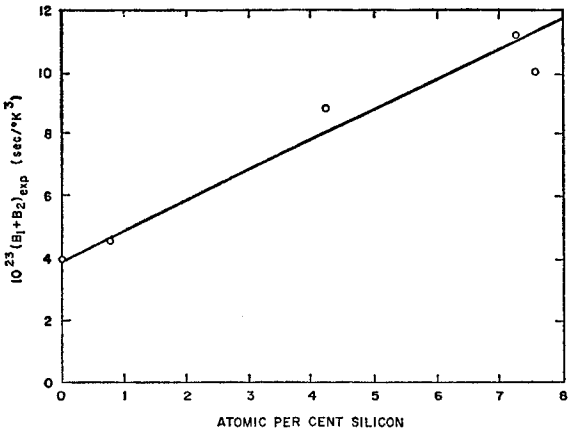

FIG. 5. Variation of $(B_1+B_2)_{exp}$ with silicon concentration.

[11] J. A. Carruthers, T. H. Geballe, H. M. Rosenberg, and J. M. Ziman, Proc. Roy. Soc. (London) **A238**, 502 (1957).
[12] E. Fagen, J. Goff, and N. Pearlman, Phys. Rev. **94**, 1415 (1954).
[13] N. Pearlman and J. F. Goff, Bull. Am. Phys. Soc. 4, 410 (1959).
[14] R. Berman, F. E. Simon, and J. M. Ziman, Proc. Roy. Soc. (London) **A220**, 171 (1953).
[15] R. Berman, E. L. Foster, and J. M. Ziman, Proc. Roy. Soc. (London) **A231**, 130 (1955).

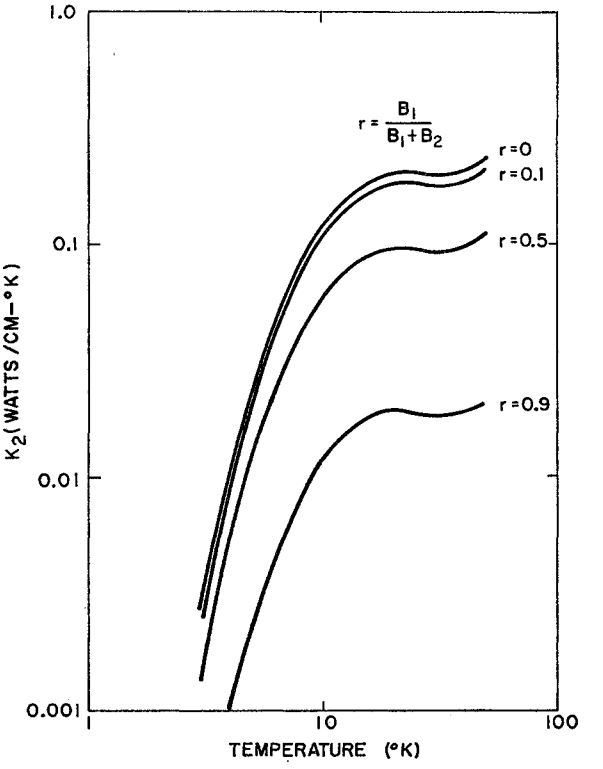

FIG. 6. The magnitude and temperature dependence of $K_2=k\beta I_2/2\pi^2 c$. The calculations shown are for germanium with B_1+B_2 set equal to 2.77×10^{-23} sec/°K^3.

scattering is specular. In this connection it is of interest to note that all of the specimens had smooth, shiny surfaces. All were etched in *CP*-4 previous to being soldered to heater and heat sink. It is not clear, however, why the Ge specimen should exhibit partial specular scattering when the other specimens apparently did not. For specimens No. 2 and No. 4, containing 0.77 at. % Si and 7.25 at. % Si, the values for c/L which gave the best fit to the data were equal to the values computed from the specimen dimensions.

In Callaway's expression for the thermal conductivity, given in Eq. (9) of this paper, there occurred two contributions, i.e., $K=K_1+K_2$, where K_1 is equal to $kI_1/2\pi^2 c$ and K_2 is equal to $k\beta I_2/2\pi^2 c$. Calculations of K_1 and K_2 on the IBM 704 indicate that for the specimens discussed here K_2 is negligible compared to K_1. In Fig. 6 are shown plots of K_2 calculated for specimen 1, pure germanium, for which K_1/K_2 is a minimum. The various curves correspond to different values for $r=B_1/(B_1+B_2)$. The parameter r is a measure of the relative importance of Umklapp and N processes. For $r=1$, $B_2=0$ and N processes are unimportant, in which case $K_2=0$. For $r=0$, $B_1=0$, which implies that Umklapp processes are unimportant and gives an upper bound for K_2 (for a given value of B_1+B_2). Comparison of these curves to $C1$ of Fig. 2 indicates that K_2 is at most 4% as large as K_1.

As a final observation, it is interesting to note a relationship between the variational calculation of Berman *et al.* and Callaway's calculation. It can easily be shown from Callaway's Eq. (24) that the thermal conductivity in the limit of low temperatures for an infinite crystal, i.e., one with no boundary scattering, is given by the expression

$$K=\frac{k}{4\pi c}\frac{1}{[A(B_1+B_2)T^3]^{\frac{1}{2}}}. \tag{16}$$

If we substitute Klemens' expression for A, $V_0\Gamma/4\pi c^3$ into Eq. (16), we obtain the result

$$K=k\Big/\left[\frac{4\pi V_0\Gamma}{c}(B_1+B_2)T^3\right]^{\frac{1}{2}}. \tag{17}$$

It is interesting to note the similarity between Eq. (17) and Eq. (8). By equating Eqs. (17) and (8), one can obtain a relationship between (B_1+B_2) and γ.

$$B_1+B_2=\gamma^2k^5/[4(0.318)^2h^2c^5MV_0]. \tag{18}$$

If we substitute into Eq. (18), the appropriate constants for germanium and take $\gamma=1.42$, we obtain $(B_1+B_2)=3.18\times10^{-23}$ sec/°K^3 which agrees within 12% with Callaway's value of 2.77×10^{-23} sec/°K^3 and within 25% with the value in Table II.

V. SUMMARY OF CONCLUSIONS

By comparing the thermal conductivities computed from the theoretical models of Klemens, Berman *et al.*, and Callaway to the thermal conductivities measured for specimens 1 through 5 whose compositions are listed in Table I, the following conclusions were reached:

1. The good agreement between the experimental data and the predictions of the models of Callaway and Klemens in the low-temperature region (i.e., at temperatures below that at which the maximum conductivity occurs) suggests the validity of the relevant assumptions made in the derivation and application of the models. These assumptions are:

(a) The silicon and germanium atoms scatter phonons as isotopic point defects with a relaxation time given by the expression derived by Klemens.

(b) The scattering of phonons at boundary surfaces is well represented by the constant relaxation time derived by Casimir.

(c) The phonon specific heat can be adequately approximated by the Debye expression.[1,2,4]

(d) For all of the specimens, the thermal conductivities in the low-temperature region can be adequately described by postulating only the above two scattering mechanisms: boundary scattering and isotopic point-defect scattering.

2. The model which best fits the experimental thermal conductivity data in the vicinity of the con-

ductivity maxima and at temperatures above that at which the maxima occur is the model proposed by Callaway. The good agreement between Callaway's model and the experimental data in this temperature region indicates that the relaxation time for three-phonon processes in Callaway's model is correct for germanium and dilute germanium-silicon alloys. In this temperature region, Klemens' model does not fit the data well. This was pointed out by the author in a previous paper.[16] The model of Berman *et al.*[3] predicts fairly well the thermal conductivities of the specimens at the highest temperatures if one chooses for γ, the Grüneisen constant, a value of 1.42. However, because the model does not take into account boundary scattering, one cannot expect to get agreement with the data in the vicinity of the conductivity maxima or at temperatures below that at which the maxima occur. In summary, of the three models considered, the one which best fits the experimental data over the entire temperature range considered, 2–50°K, is the model proposed by Callaway.

3. There is strong evidence for the existence in the alloy specimens of internal boundaries which can scatter phonons in the same manner as the external surfaces. These internal boundaries are believed to be associated with microscale fluctuations in composition previously reported by Goss, Benson, and Pfann.

ACKNOWLEDGMENTS

The author is indebted to Professor R. L. Sproull of Cornell University for many helpful discussions; to Dr. W. Reuter of the IBM Research Center for spectroscopic analysis of the germanium specimen; and to Mrs. M. Charap and George Chang of the IBM Research Center for their help in numerically evaluating integrals on the IBM 704 computer.

APPENDIX. DISCUSSION OF PLANAR DEFECTS

It is clear from Figs. 1 and 4, that in order to fit any of the models under discussion to the alloy specimen containing Ge+7.56 at. % Si, one must use a value for c/L which is at least five times larger than for any of the other specimens, including the one containing Ge+7.25 at. % Si. Since it is extremely unlikely that the phonon velocity varies much from specimen to specimen, it follows that L, the mean free path for boundary scattering, must be about five times smaller for this specimen, even though it is the same size as the other specimens.

It was pointed out by Goss, Benson, and Pfann[17] that microscale fluctuations of solute concentration occur in Ge-Si alloy crystals grown from the melt. These are revealed by grinding the specimen surface and etching with *CP*-4. Because etch rate varies with composition, fluctuations in silicon concentration are manifested as surface striae lying parallel to interface positions. In a specimen of Ge+6 at. % Si, Goss, Benson, and Pfann also observe dislocation etch pits lined up parallel to the striae. They infer that for a discontinuity in solute concentration of perhaps 0.1 at. % or more, an array of edge dislocations may be expected.

It seems quite likely that the planar interfaces between regions differing in solute concentration would scatter phonons. Further, it is likely that the scattering would be similar in nature to that which occurs at crystal boundaries, i.e., it would manifest itself by a decrease in L (or an increase in c/L). To see whether such fluctuations in solute concentration occur in the specimens under discussion, they were etched in *CP*-4 and examined. In Figs. 7 to 11 are shown some of the results.

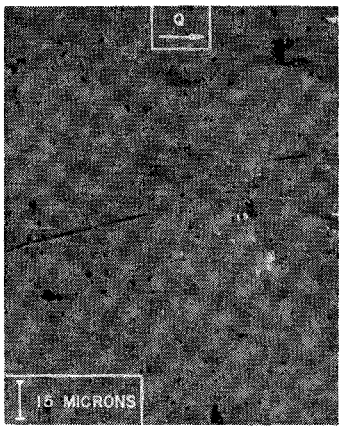

FIG. 7. Bright-field photomicrograph of etched surface of Ge+0.77 at. % Si sample. The interval indicated on the photograph is equivalent to 15 microns on specimen. Arrow indicates direction of heat flow during thermal conductivity measurements.

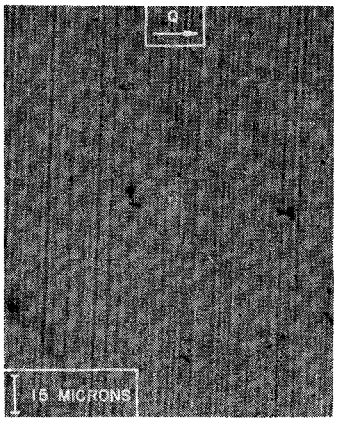

FIG. 8. Bright-field photomicrograph of etched surface of Ge+4.23 at. % Si sample. The interval indicated on the photograph is equivalent to 15 microns on specimen. Arrow indicates direction of heat flow during thermal conductivity measurements.

[16] A. M. Toxen, Phys. Rev. **110**, 585 (1958).
[17] A. J. Goss, K. E. Benson, and W. G. Pfann, Acta Met. 4, 332 (1956).

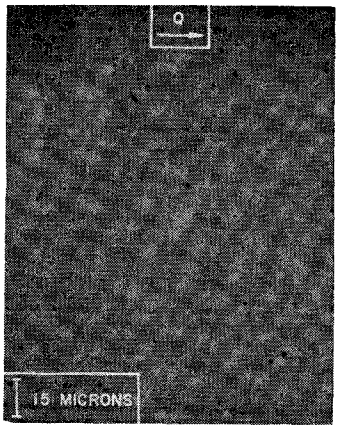

FIG. 9. Bright-field photomicrograph of etched surface of Ge+7.25 at. % Si sample. The interval indicated on the photograph is equivalent to 15 microns on specimen. Arrow indicates direction of heat flow during thermal conductivity measurements.

All of the alloy specimens show striae. In Figs. 7 to 10 are bright field photographs of the specimens: 0.77 at. % Si, 4.23 at. % Si, 7.25 at. % Si, and 7.56 at. % Si, respectively. The arrow marked Q shows the direction of heat flow during the thermal conductivity measurements. The Ge specimen showed no evidence of striae. In addition to the striae, the 7.56 at. % Si specimen exhibited etch pits lined up parallel to the striae. None of the other specimens showed this feature.

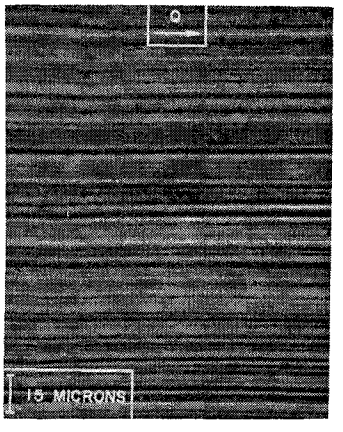

FIG. 10. Bright-field photomicrograph of etched surface of Ge+7.56 at. % Si sample. The interval indicated on the photograph is equivalent to 15 microns on specimen. Arrow indicates direction of heat flow during thermal conductivity measurements.

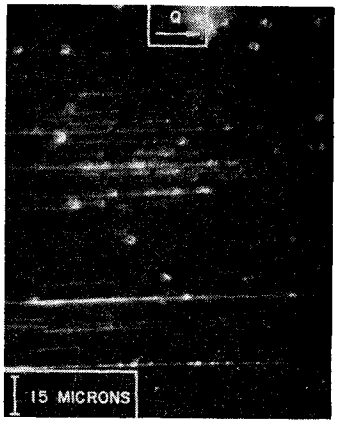

FIG. 11. Dark-field photomicrograph of Ge+7.56 at. % Si. The interval indicated on the photograph is equivalent to 15 microns on specimen. Arrow indicates direction of heat flow during thermal conductivity measurements.

This is shown best in Fig. 11 which is a dark-field photomicrograph of the 7.56 at. % Si specimen.

Since the 7.56 at. % Si specimen exhibits the most prominent striae as well as the arrays of dislocations, it seems reasonable to conclude that in this specimen the fluctuations in silicon concentration are the most extreme. Hence, if the interfaces between regions of differing silicon concentration scatter phonons, the effect should be most prominent in this specimen. Indeed, it is just for this specimen that it was necessary to increase c/L by a factor of five from the expected value to account for the observed thermal conductivity.

The specimen with the next most prominent striae was that containing 4.23 % Si. In addition, in this specimen the direction of heat flow in thermal conduction measurements was normal to the interfaces, whereas the heat flow was parallel to the interfaces for the other specimens. It is therefore significant that for this specimen also an increase of c/L improved the fit of the theoretical curve to the experimental data.

The nonuniform distribution of the silicon would have an additional effect. The values for A used in calculating the theoretical curves of Figs. 1, 2, and 3 were calculated under the assumption that the silicon was homogeneously distributed. Any deviation from the homogeneous distribution would result in smaller values for A. This is the observed deviation as is evident from a comparison of Table I with Table II.

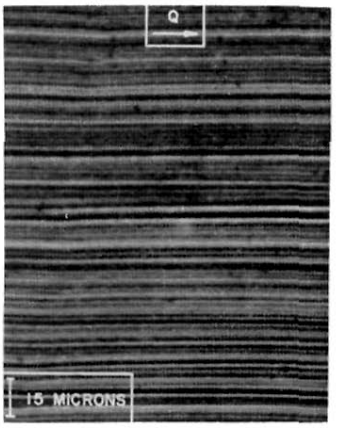

FIG. 10. Bright-field photomicrograph of etched surface of Ge+7.56 at. % Si sample. The interval indicated on the photograph is equivalent to 15 microns on specimen. Arrow indicates direction of heat flow during thermal conductivity measurements.

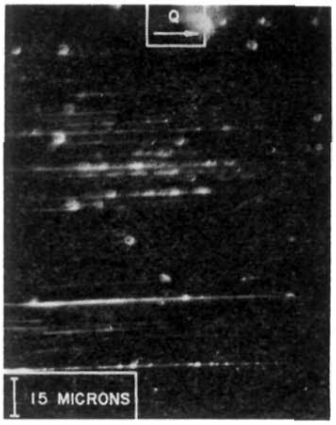

FIG. 11. Dark-field photomicrograph of Ge+7.56 at. % Si. The interval indicated on the photograph is equivalent to 15 microns on specimen. Arrow indicates direction of heat flow during thermal conductivity measurements.

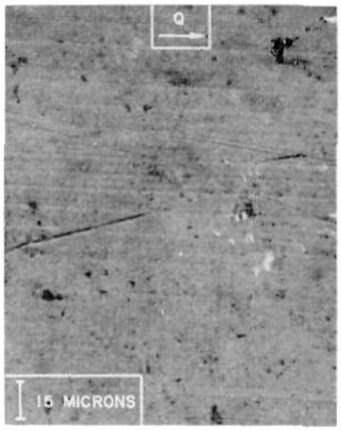

FIG. 7. Bright-field photomicrograph of etched surface of Ge+0.77 at. % Si sample. The interval indicated on the photograph is equivalent to 15 microns on specimen. Arrow indicates direction of heat flow during thermal conductivity measurements.

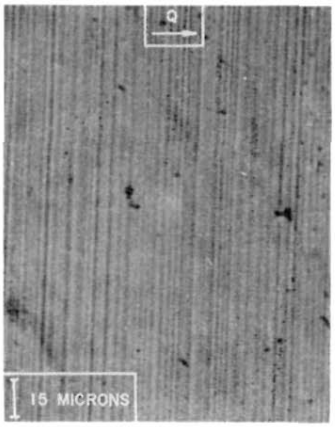

FIG. 8. Bright-field photomicrograph of etched surface of Ge+4.23 at. % Si sample. The interval indicated on the photograph is equivalent to 15 microns on specimen. Arrow indicates direction of heat flow during thermal conductivity measurements.

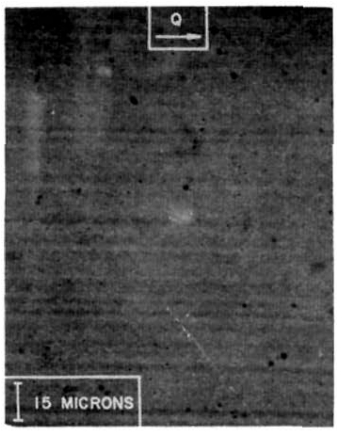

FIG. 9. Bright-field photomicrograph of etched surface of Ge+7.25 at. % Si sample. The interval indicated on the photograph is equivalent to 15 microns on specimen. Arrow indicates direction of heat flow during thermal conductivity measurements.